Supplemental Material for: Observation of Quadratic (Charge-2) Weyl Point Splitting in Near-Infrared Photonic Crystals

Christina Jörg,[1,2,*] Sachin Vaidya,[1,*] Jiho Noh,[3] Alexander Cerjan,[1,4,5]
Shyam Augustine,[2] Georg von Freymann,[2,6] and Mikael C. Rechtsman[1]

[1] *Department of Physics, The Pennsylvania State University, University Park, Pennsylvania 16802, USA*
[2] *Physics Department and Research Center OPTIMAS, University of Kaiserslautern, D-67663 Kaiserslautern, Germany*
[3] *Department of Mechanical Science and Engineering, University of Illinois at Urbana-Champaign, Urbana, Illinois 61801, USA*
[4] *Sandia National Laboratories, Albuquerque, New Mexico 87185, USA*
[5] *Center for Integrated Nanotechnologies, Sandia National Laboratories, Albuquerque, New Mexico 87185, USA*
[6] *Fraunhofer Institute for Industrial Mathematics ITWM, 67663, Kaiserslautern, Germany*

(Dated: November 2, 2021)

CONTENTS

I. Measurements and simulations along $\mathbf{\Gamma} - \mathbf{Y}$ 2

II. Sample parameters 2

III. Accidental quadratic Weyl points 3

IV. Coupling analysis 3

V. Weyl point at $\mathbf{R}$ 4

References 5

---

* These two authors contributed equally.

I. MEASUREMENTS AND SIMULATIONS ALONG Γ – Y

In addition to the spectra taken along the $\mathbf{\Gamma} - \mathbf{X}$ direction, we also performed measurements and simulations along $\mathbf{\Gamma} - \mathbf{Y}$, which are shown in Fig. S1. We see here that the two bands, which form the quadratic WP for equal rod widths in all layers, move apart upon increasing w_0 and are no longer degenerate. This is as expected since the linear WPs are point degeneracies that only occur along the $\mathbf{\Gamma} - \mathbf{X}$ direction.

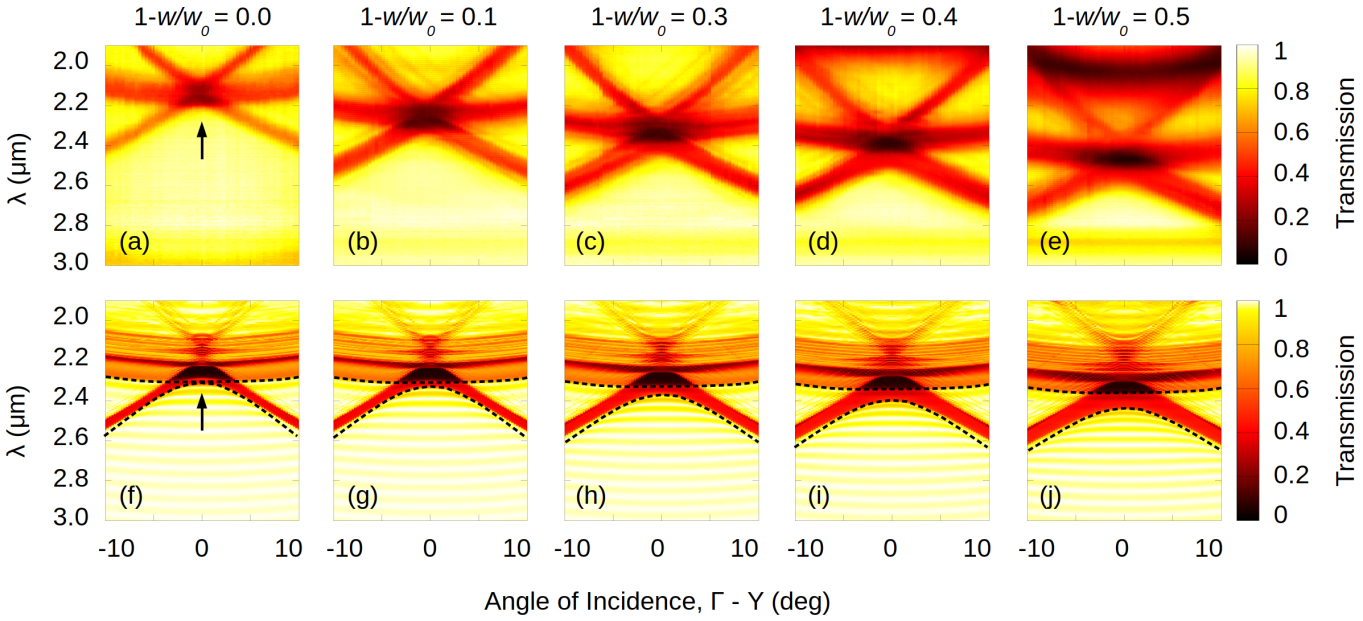

FIG. S1. Spectra along $\mathbf{\Gamma} - \mathbf{Y}$: (a)-(e) Measured angle-resolved FTIR spectra of the chiral woodpile PhC with varying values of the width w_0. (f)-(j) The corresponding RCWA simulated spectra of the chiral woodpile PhC. The dashed black lines are bulk bands calculated from MPB. We see that the two bands that form the quadratic WP for $w = w_0$ move apart on increasing rod width w_0.

II. SAMPLE PARAMETERS

The structural parameters of the woodpile photonic crystal (PhC) samples, as determined by SEM, are given in table I .

Fig.	w (μm)	w_0 (μm)	a (μm)
3 (a)	0.15 ± 0.01	0.14 ± 0.01	2.0 ± 0.1
3 (b), 4	0.20 ± 0.02	0.22 ± 0.01	2.1 ± 0.1
3 (c), 4	0.19 ± 0.01	0.26 ± 0.02	2.1 ± 0.1
3 (d), 4	0.20 ± 0.01	0.35 ± 0.01	2.1 ± 0.2
3 (e), 4	0.23 ± 0.02	0.43 ± 0.05	2.0 ± 0.1
4	0.18 ± 0.02	0.24 ± 0.02	2.1 ± 0.1
4	0.19 ± 0.03	0.24 ± 0.01	2.1 ± 0.1
4	0.19 ± 0.02	0.25 ± 0.02	2.0 ± 0.1
4	0.21 ± 0.01	0.45 ± 0.01	2.1 ± 0.1

TABLE I. Structural parameters of the samples used in Fig. 3 and Fig. 4 in the main text as determined by SEM.

Horizontal error bars in Fig. 4 of the main text are a result of propagation of the individual errors of w and w_0 as given in Table I. Vertical error bars in Fig. 4 are assumed to be 2 pixels wide, which corresponds to 0.72°, since we read off the position of the split WPs from the angle-resolved spectra. Therefore, θ is the difference between the two angles of incidence, as plotted on the horizontal axis in Fig. 3, at which the split WPs are located.

III. ACCIDENTAL QUADRATIC WEYL POINTS

As stated in the main text, the momentum space separation of the WPs is not generally a monotonic function of the symmetry-breaking parameter, $1 - w/w_0$. We present an example of an accidental quadratic WP which is formed due to the re-merging of the split linear WPs on increasing the symmetry-breaking parameter. The band structure for a chiral woodpile made out of Si rods ($\varepsilon = 12$) is shown in Fig. S2. For $w_0 = w$ we have the quadratic WP, protected by screw symmetry (Fig. S2 (a)). As with the low-contrast PhC in the experiment, upon increasing w_0, this quadratic WP splits into two linear WPs, whose separation first increases along the $\mathbf{\Gamma} - \mathbf{X}$ direction (Fig. S2 (b)). However, increasing w_0 further causes their separation to decrease to zero (Fig. S2 (c)), leading to the formation of an accidental quadratic WP. Increasing w_0 beyond this re-merging point leads to a splitting of this quadratic WP along a different symmetry-allowed direction, $\mathbf{\Gamma} - \mathbf{Y}$ in this case (Fig. S2 (d)).

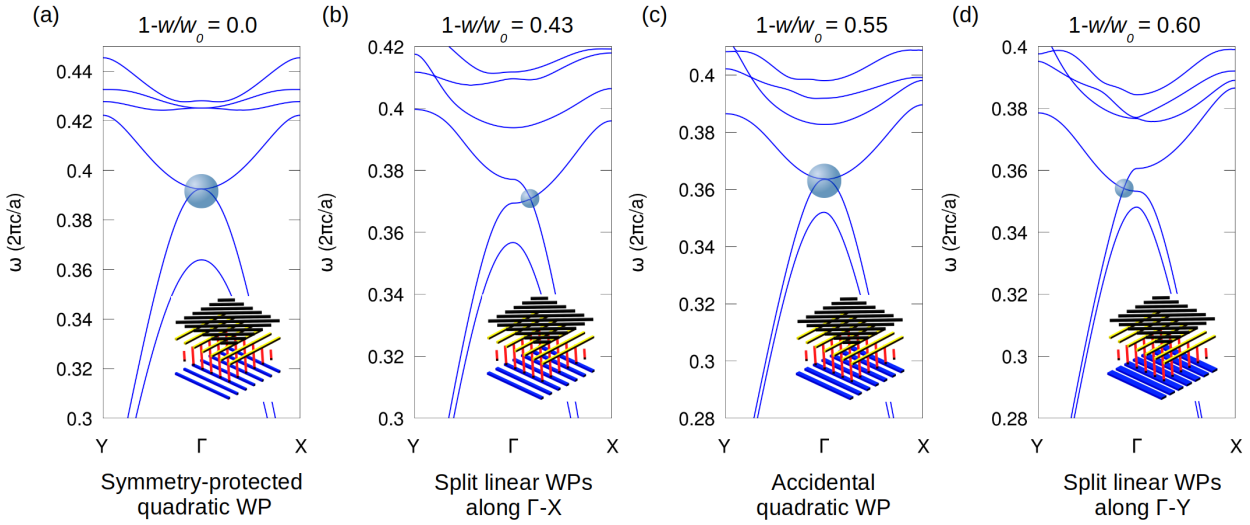

FIG. S2. (a) Symmetry-protected quadratic WP for $w_0 = w$. (b) This quadratic WP first splits into two linear WPs along $\mathbf{\Gamma} - \mathbf{X}$ upon increasing w_0. (c) Further increasing w_0 re-merges the two linear WPs, leading to the formation of an accidental quadratic WP. (d) Increasing w_0 beyond the re-merging point leads to a splitting of this quadratic WP along $\mathbf{\Gamma} - \mathbf{Y}$.

IV. COUPLING ANALYSIS

In the experiment presented in the main text, the WPs are embedded inside a continuum of states of other projected bands of the PhC. Despite this, we are able to observe the WPs and $k_z = 0$ Weyl bands as the boundaries of spectral features where the transmission drops sharply to zero. Here, we explain this observation by performing a coupling analysis similar to [1–5]. Two coefficients, C_s and C_p, and mode coupling index, κ, are defined using the overlap integrals between s-polarized (p-polarized) plane waves $|s(p)\rangle$ and the Bloch modes of the PhC $|\psi_{n,\mathbf{k}}(x,y,z)\rangle$ with momentum $\mathbf{k}$ and band index n:

$$\eta_{s(p)} = |\langle s(p)|\psi_{n,\mathbf{k}}(x,y,z)\rangle|^2, \qquad \kappa = \eta_s + \eta_p, \qquad C_{s(p)} = \eta_{s(p)}/\kappa. \tag{S1}$$

The coefficient $C_{s(p)}$ ($0 \leq C_{s(p)} \leq 1$) measures the degree of coupling between the polarized plane waves and the Bloch modes of the PhC while κ ($0 \leq \kappa \leq 1$) measures the strength of coupling to a plane wave of any arbitrary polarization. Vanishingly small transmission in the spectrum in the absence of bandgaps can be thought of as either a polarization mismatch between the incident wave and the modes of the PhC, indicated by small $C_{s(p)}$, and/or inefficient mode in-coupling, indicated by small κ.

In Fig. S3, we analyze the cut of the transmission spectra for each polarization at $\mathbf{\Gamma}$ for a PhC with parameters corresponding to Fig. 3 (h) of the main text. The band structure along the projected momentum k_z, for $\mathbf{k}_{\|} = \mathbf{\Gamma}$, are shown in Fig. S3 (a) and (c). Here, the states are characterized by the values of $C_{s(p)}$ and κ. The RCWA simulations of the s- and p- polarized spectra are shown in Fig. S3 (b). We can see that the sharp drop in transmission at $\mathbf{\Gamma}$ around 2.4 µm for both polarizations is a result of a polarization mismatch and/or poor mode in-coupling of the Bloch modes (highlighted in blue in Fig. S3 (a) and (c)). The boundaries of these spectral features in each polarization

match the two $k_z = 0$ Weyl bands, allowing for a direct observation of WPs in the spectrum of 45°-polarized light. In the experiment we measure the spectrum of unpolarized light which is similar to that of 45°-polarized light as can be seen from the experimentally obtained polarized spectrum plotted in Fig. S3 (d)-(g). Simulations away from $\mathbf{k}_{\|} = \mathbf{\Gamma}$ show that this analysis continues to hold, allowing for this relatively unobscured observation of the splitting of WPs.

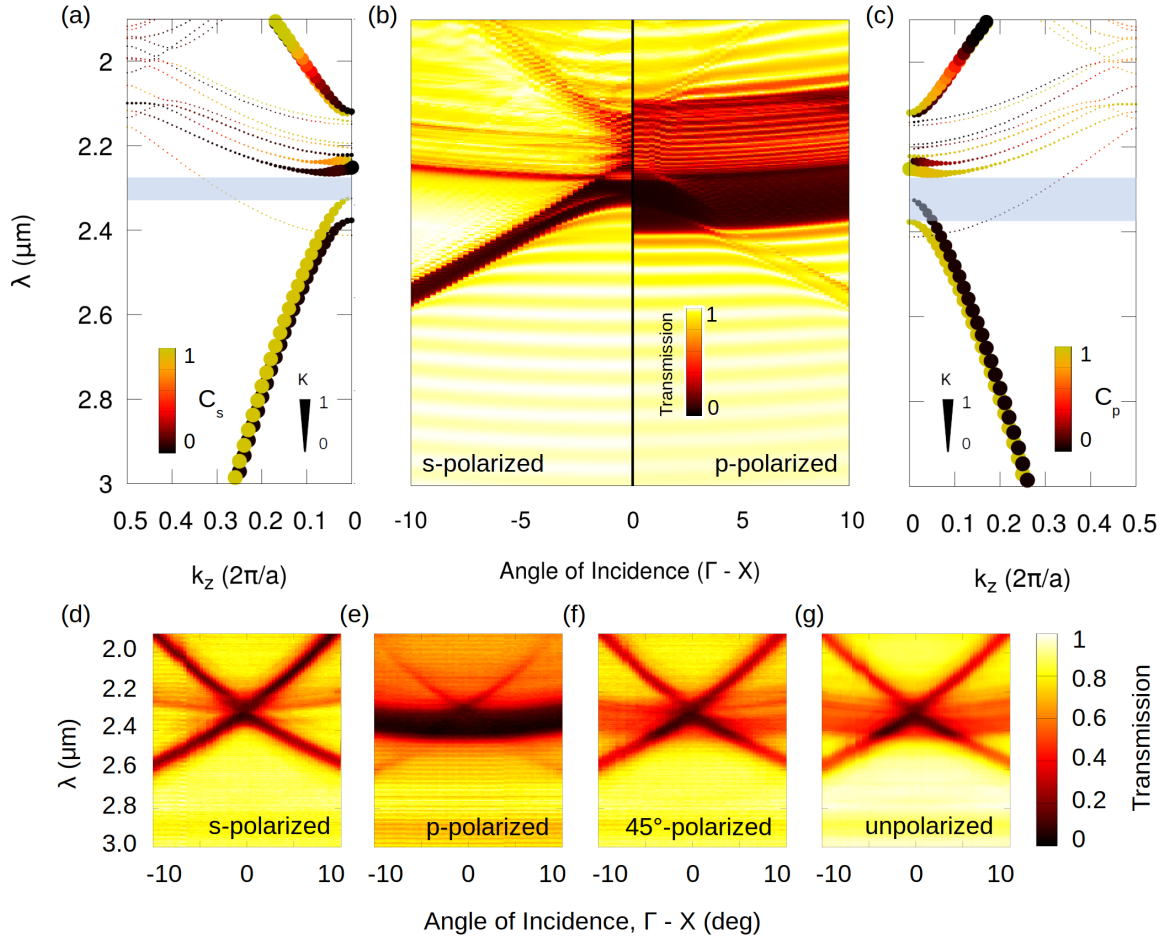

FIG. S3. (a), (c) The band structure showing bands 3 to 18 for $\mathbf{k} = (0, 0, k_z)$. The color of the circular dots indicates the value of $C_{s(p)}$ and their size is proportional to the value of κ for the corresponding Bloch modes. The blue highlighted region shows a band of wavelengths with polarization mismatch and/or poor mode in-coupling, leading to the observed sharp drop in transmission at $\mathbf{k}_{\|} = \Gamma$. The large-wavelength boundaries of these features correspond to bands 5 and 4 at $k_z = 0$ for s and p polarizations, respectively. (b) The RCWA simulated s- and p-polarized transmission spectra with parameters corresponding to Fig. 3 (h) of the main text. (d)-(g) Experimentally measured transmission spectra for s-polarized, p-polarized, 45°-polarized and unpolarized light, respectively.

V. WEYL POINT AT R

The partner WP to the one at $\mathbf{\Gamma}$ is also a symmetry protected WP but of charge -2 and is located at the corners of the 3D Brillouin zone ($\mathbf{R}$ point). The dispersion around this WP and a plot of the Berry phase calculated on a sphere enclosing it is shown in Fig. S4. For low dielectric contrast such as in our experiment, this WP lies close to but slightly above the light line. However, the large angle of incidence required ($\sim 80°$) and low transmission of the PhC near the edge of the light line makes it impractical for measurement. To remedy this, period-doubling via gratings or perturbations to the structure could be employed to move this WP to smaller angles of incidence.

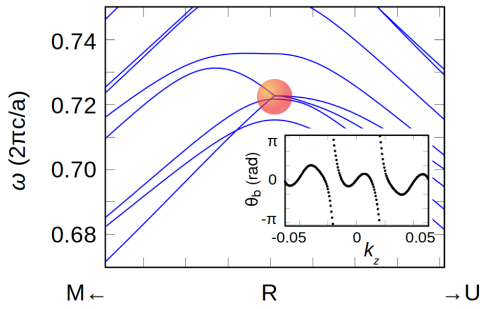

FIG. S4. Band structure of the chiral woodpile PhC in the vicinity of the **R** point, made out of dielectric rods ($\varepsilon = 2.31$), with equal widths for all rods. The quadratic WP is marked with a red circle. The inset shows a plot of the winding of the Berry phase for band 4 in a sphere around **R**. The double winding indicates that the degeneracy has a charge of -2.

[1] T.-H. Kao, L.-Y. C. Chien, and Y.-C. Hung, Opt. Express **23**, 24416 (2015).
[2] I. Karakasoglu, M. Xiao, and S. Fan, Opt. Express **26**, 21664 (2018).
[3] M. Saba, M. Thiel, M. D. Turner, S. T. Hyde, M. Gu, K. Grosse-Brauckmann, D. N. Neshev, K. Mecke, and G. E. Schröder-Turk, Phys. Rev. Lett. **106**, 103902 (2011).
[4] S. Takahashi, T. Tajiri, Y. Ota, J. Tatebayashi, S. Iwamoto, and Y. Arakawa, Applied Physics Letters **105**, 051107 (2014).
[5] S. Vaidya, J. Noh, A. Cerjan, C. Jörg, G. von Freymann, and M. C. Rechtsman, Phys. Rev. Lett. **125**, 253902 (2020).